Engineering Knill–Laflamme–Milburn Entanglement via Dissipation and Coherent Population Trapping in Rydberg Atoms

Rui Li(李芮)[1], Shuang He(何爽)[2], Zhi-Jun Meng(孟枳君)[1], Zhao Jin(金钊)[3], and Wei-Jiang Gong(公卫江)[1*]

[1]*College of Sciences, Northeastern University, Shenyang 110819, China*
[2]*Aviation University of Air Force, Changchun 130022, China*
[3]*NCO School, Army Academy of Artillery and Air Defense, Shenyang 110867, China*

(Received 10 March 2023; accepted manuscript online 15 May 2023)

We present a scheme for dissipatively preparing bipartite Knill–Laflamme–Milburn (KLM) entangled state in a neutral atom system, where the spontaneous emission of excited Rydberg states, combined with the coherent population trapping, is actively exploited to engineer a steady KLM state from an arbitrary initial state. Instead of commonly used antiblockade dynamics of two Rydberg atoms, we particularly utilize the Rydberg–Rydberg interaction as the pumping source to drive the undesired states so that it is unnecessary to satisfy a certain relation with laser detuning. The numerical simulation of the master equation signifies that both the fidelity and the purity above 98% is available with the current feasible parameters, and the corresponding steady-state fidelity is robust to the variations of the dynamical parameters.

DOI: 10.1088/0256-307X/40/6/060302

Entanglement as one of the most pivotal characteristics in quantum information theory reveals significant insights into nonlocality and nonclassical correlations. Genuinely entangled pure state is usually an ideal resource in the progress of quantum science and technology, such as quantum key distribution,[1–3] Bell's inequalities,[4–6] quantum teleportation,[7–10] and dense coding.[11–13] Among various types of entangled qubits, Knill–Laflamme–Milburn (KLM) states[14] have been demonstrated to be an efficient ancilla for enhancing the success probability of teleportation-based quantum computing with the increase in qubits. As described in the previous works, a KLM state is a distinct class of entangled multiparticle states, which is usually defined as the superposition of respective basic states.[15] Another essential feature is that its entanglement is highly robust against the qubit loss, even in the absence of anyone of qubits, the remaining particles are still entangled, as opposed to a usual Greenberger–Horne–Zeilinger state.[16,17] Since then, much effort has been devoted to preparation of the KLM-type quantum entanglement with different physical platforms, e.g., linear optics,[18] atom-cavity quantum electrodynamics,[19–21] nonlinear cross-Kerr medium,[22] and artificial atom.[23] Moreover, direct conversion from other kinds of entanglement to a KLM state is also an interesting issue for the state preparation, which has been achieved in atomic, ionic, and optical systems.[24–28]

Unfortunately, dissipation is always detrimental to quantum information processing tasks, because of the decoherent effect arising from the inevitable coupling between the quantum system and its environment, especially in the prime stage of entanglement preparation, making the system become of mixed states.[29,30] However, quantum reservoir engineering is an alternative approach that involves tailoring dissipative processes or utilizing decoherence to manipulate quantum systems.[31,32] Optical pumping and laser cooling are typical methods to promote removal of entropy and to stabilize the system into the target state from an uncontrolled and unknown initial state, which is not available by unitary dynamics alone. Recently, much attention has been paid using dissipation for generating entanglement. In particular, Zou *et al.*[33] theoretically investigated the dissipative coupling and preparation of entangled two-qubit spin states (Bell states) induced by a generic noisy magnetic medium in a hybrid quantum system. Cole *et al.*[34] discussed a scheme that uses sympathetic cooling as the dissipation mechanism and relies on tailored destructive interference to generate anyone of six entangled W states in a three-ion qubit space. Furthermore, dissipative preparation has been generalized to high-dimensional,[35,36] multipartite,[37–41] and distant entanglements.[42] According to the previous reports, dissipative preparation has been realized in various experimental platforms, including superconductors,[43,44] photons,[45,46] quantum dots,[47] nitrogen-vacancy centers,[48] neutral atoms,[49,50] and trapped ions.[51]

Neutral atoms are known to be an appealing candidate among numerous physical systems due to the long-lived encoding in atomic hyperfine states and extremely large dipole moments. Particularly, the last character can block the simultaneous population of multiple Rydberg states over a separation relative to the atomic scale,[52,53] leading to Rydberg blockade. Combined with this effect, fast quantum logic gates,[54] quantum simulators,[55] quantum algorithms,[56] and quantum repeaters[57] have been theoretically implemented. Unlike the Rydberg blockade, the Rydberg antiblockade regime[58] shows better superiority for dissipative preparation of entangled states,[59] owing to the interaction-induced excitation enhancement.

*Corresponding author. Email: gwj@mail.neu.edu.cn
© 2023 Chinese Physical Society and IOP Publishing Ltd

Especially, Li *et al.*[60] have reviewed the Rydberg antiblockade regimes with different types and strengths of Rydberg–Rydberg interaction (RRI), followed by the discussion of their applications. Motivated by these progress, researchers devote themselves to the fast and dephasing-tolerant preparation of steady KLM states via dissipative Rydberg pumping.[15] Following these works, in this Letter we present an alternative concrete scheme for the dissipative production of bipartite KLM state involving the single-atom dark state induced by the the coherent population trapping. Our scheme has the following characteristics: (i) In contrast to the Rydberg-antiblock-based dissipative schemes,[61,62] the RRI between two Rydberg atoms is particularly utilized as pumping source to drive the undesired states to high-excitation subspace, i.e., the scheme works under the blockade condition, so that the RRI does not need to satisfy a certain relation with laser detuning. (ii) Over time, the results show that the purity and fidelity of the target state are close to 1, and the corresponding steady-state fidelity is robust to the variations of the dynamical parameters. (iii) This idea makes spontaneous atomic emission a favorable resource. The preparation of KLM entangled states can be realized without state initialization and precise evolution time.

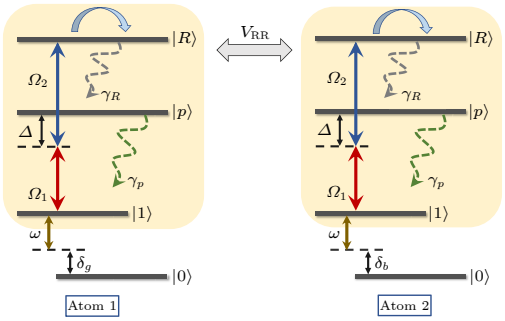

Fig. 1. Energy-level structure of two Rydberg atoms. The ground-state levels $|0\rangle$ and $|1\rangle$ are coupled by a microwave field with Rabi frequency ω_j ($j = a,\ b$) and detuning δ. The Rydberg state $|R\rangle$ is driven from the ground state $|1\rangle$ by a resonant two-photon process via the intermediated short-lived excited level $|p\rangle$. Ω_1 and Ω_2 denote the Rabi frequencies of the transitions $|1\rangle \leftrightarrow |p\rangle$ and $|p\rangle \leftrightarrow |R\rangle$, respectively, and Δ is the corresponding detuning. $V_{\rm RR}$ stands for the interatomic Rydberg interaction strength, γ_R and γ_p represent the atomic spontaneous emission rates of $|R\rangle$ and $|p\rangle$, respectively, where $\gamma_R \ll \gamma_p$ is satisfied.

Basic Model. As shown in Fig. 1, two ladder-type four-level ^{87}Rb atoms are confined in spatially separated dipole traps at a distance less than 10 μm.[52] Each of the atoms has two ground states, i.e., $|0\rangle$ and $|1\rangle$, a short-lived intermediate state $|p\rangle$ and a long-lived Rydberg excited state $|R\rangle$. A pair of red and blue sideband laser fields with corresponding Rabi frequencies Ω_1 and Ω_2 are applied to drive the transitions $|1\rangle \to |p\rangle$ and $|p\rangle \to |R\rangle$, respectively. The nonresonant coupling between ground states $|0\rangle$ and $|1\rangle$ of atom 1 (atom 2) is realized by microwave field or Raman transition with Rabi frequency $\omega_{a(b)}$ and detuning δ. Here, as a typical case, we would like to take $\delta_a = -\delta_b = \delta$,[63] and the Rydberg state $|R\rangle$ (intermediate state $|p\rangle$) can spontaneously decay to $|0\rangle$ and $|1\rangle$ with the same rate γ_R (γ_p), respectively. In addition, the interaction between Rydberg atoms originates from the strong long-range dipole-dipole potential. On the scale of van der Waals domain, the state is $V_{\rm RR} = C_6/r^6$ with r being the interatomic separation and C_6 the dispersion coefficient depending on the quantum numbers of the Rydberg state. The Hamiltonian for the current system, in the interaction picture, is given by ($\hbar = 1$)

$$\hat{H} = \sum_{j=1,2} (\hat{H}^j_\Omega + \hat{H}^j_\omega) + \hat{H}_d, \tag{1}$$

$$\hat{H}^j_\Omega = \Delta|p\rangle_{jj}\langle p| + (\Omega_1|1\rangle_{jj}\langle p| + \Omega_2|p\rangle_{jj}\langle R| + \text{H.c.}), \tag{2}$$

$$\hat{H}^j_\omega = (\omega|0\rangle_{jj}\langle 1| + \text{H.c.}) - (-1)^j\delta|0\rangle_{jj}\langle 0|, \tag{3}$$

$$\hat{H}_d = V_{\rm RR}\ |R\rangle_{11}\langle R| \otimes |R\rangle_{22}\langle R|. \tag{4}$$

The label j represents the jth atom. In the total Hamiltonian H, we first focus on the single-atom Hamiltonian $\hat{H}^j = \hat{H}^j_\Omega + \hat{H}^j_\omega$. Note that $\hat{H}^j_\Omega$ describes a two-photon Raman resonant situation pumped by laser fields (yellow shaded regions in Fig. 1), and it would give rise to the coherent population trapping in the dark eigenstate $|D\rangle = (\Omega_2|1\rangle - \Omega_1|R\rangle)/\sqrt{\Omega_1^2 + \Omega_2^2}$. Also, one closely related result is the electromagnetically induced transparency (EIT) phenomenon. There are also two bright eigenstates $|\zeta_\pm\rangle = [2\Omega_1|1\rangle + (\Delta \pm \tilde{\Delta})|p\rangle + 2\Omega_2|R\rangle]/\mathcal{M}_\pm$ and one uncoupled dark eigenstate $|0\rangle$ belonging to the eigenspace of $\hat{H}^j_\Omega$, where $\mathcal{M}_\pm = \sqrt{4\Omega_1^2 + (\Delta \pm \tilde{\Delta})^2 + 4\Omega_2^2}$ and $\tilde{\Delta} = \sqrt{\Delta^2 + 4\Omega_1^2 + 4\Omega_2^2}$ are the normalization constant and the renormalized parameter, respectively. The corresponding eigenvalues are $E_\pm = (\Delta \pm \tilde{\Delta})/2$ and $E_0 = 0$.

If we consider a weak Raman coupling approximation between states $|0\rangle$ and $|1\rangle$, i.e., $\omega \ll \Omega_1, \Omega_2$, the single atom term $\hat{H}^j_\omega$ can be rewritten in terms of the complete orthonormal vectors $|0\rangle$, $|D\rangle$, and $|\zeta_\pm\rangle$, given as

$$\hat{H}^j_\omega = \omega\Big(\frac{\Omega_2}{\sqrt{\Omega_1^2+\Omega_2^2}}|0\rangle_{jj}\langle D| + \frac{2\Omega_1}{\mathcal{M}_\pm}|0\rangle_{jj}\langle\zeta_\pm|e^{-iE_\pm t} + \text{H.c.}\Big) - (-1)^j\delta|0\rangle_{jj}\langle 0|. \tag{5}$$

The high-frequency oscillating terms proportional to $\exp(-iE_\pm t)$ can be neglected when the limiting condition $E_\pm \gg 0$ is satisfied. Then, it is reasonable to replace the bare-state coupling $|0\rangle_j \leftrightarrow |1\rangle_j$ by performing an effective resonant transition between the eigenstates $|0\rangle_j$ and $|D\rangle_j$.

In addition to Hamiltonian dynamics, atomic spontaneous emission also plays a crucial role. The evolution of the system in this case is modeled by the Lindblad–Markovian master equation,[22] i.e.,

$$\dot{\hat{\rho}} = i[\hat{\rho}, H] + \frac{1}{2}\sum_j \big[2\hat{\mathcal{L}}_j\hat{\rho}\hat{\mathcal{L}}_j^\dagger - (\hat{\mathcal{L}}_j^\dagger\hat{\mathcal{L}}_j\hat{\rho} + \hat{\rho}\hat{\mathcal{L}}_j^\dagger\hat{\mathcal{L}}_j)\big]. \tag{6}$$

$\hat{\mathcal{L}}_j$ is the so-called Lindblad operators governing dissipation. Specifically, in the current scheme the Lindblad operators can be expressed as $\hat{\mathcal{L}}^0_j = \sqrt{\gamma_p/2}|0\rangle_{jj}\langle p|$ and $\hat{\mathcal{L}}^1_j = \sqrt{\gamma_p/2}|1\rangle_{jj}\langle p|$, which describe the decay induced by the spontaneous emission of the jth atom. Since the Rydberg state is long lived, the dissipative process from the Rydberg state to intermediate level corresponds to a relatively slow dynamics ($\gamma_R \ll \gamma_p$), so we ignore the effect of $\sqrt{\gamma_R/2}|p\rangle_{jj}\langle R|$ in the following discussions.

Table 1. The eigenstates and eigenenergies of the Hamiltonian $\sum_{j=1,2}\hat{H}_{\Omega}^{j}$ within the two-excitation subspace.

Eigenstate	Eigenenergy
$\|00\rangle$, $\|DD\rangle$, $\|DT\rangle$, $\|DS\rangle$	0
$\|0\zeta_{\pm}\rangle$, $\|D\zeta_{\pm}\rangle$, $\|\zeta_{\pm}D\rangle$, $\|\zeta_{\pm}0\rangle$	$(\Delta\pm\tilde{\Delta})/2$
$\|\zeta_{+}\zeta_{-}\rangle$, $\|\zeta_{-}\zeta_{+}\rangle$	Δ

Now we take into account the state space of the two-atom system spanned by the tensor product of eigenstates of $\hat{H}_{\Omega}^{j}$, as shown in Table 1, where the high-energy subspaces $|\zeta_{+}\zeta_{+}\rangle$ and $|\zeta_{-}\zeta_{-}\rangle$ have been discarded due to the perturbative transition probability caused by non-resonant excitation. According to the quantity of containing the component of the intermediary exited state ($|\zeta_{+}\rangle$ or $|\zeta_{-}\rangle$), the whole state space can be divided into three subspaces, i.e., dark singlet-triplet combination $\{|00\rangle, |DS\rangle = (|D0\rangle - |0D\rangle)/\sqrt{2}, |DT\rangle = (|D0\rangle + |0D\rangle)/\sqrt{2}, |DD\rangle\}$, single-, and two-excitation subspaces correspond to the eigenvalues 0, $(\Delta\pm\tilde{\Delta})/2$, and Δ, respectively. Using these two-atom bases, the microwave field Hamiltonian in Eq. (1) can be rewritten as

$$\sum_{j=1,2}\hat{H}_{\omega}^{j} = \sqrt{2}\omega(|00\rangle\langle DT| + |DT\rangle\langle DD|) + \delta|DT\rangle\langle DS| + \text{H.c.} \tag{7}$$

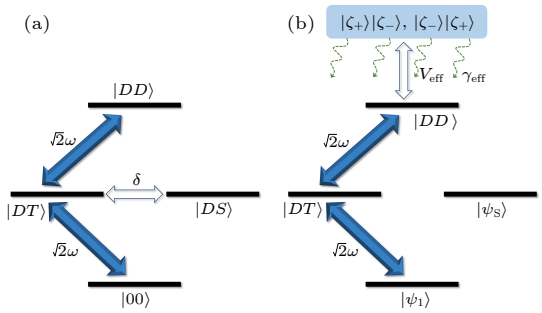

Fig. 2. (a) Effective ground state level configuration for the two-atom system and the dynamical oscillations among the collective states driven by microwave fields $\sum_{j=1,2}\hat{H}_{\omega}^{j}$ with Rabi frequency $\sqrt{2}\omega$. (b) Coherent and dissipative interactions between ground and excited states in the steady-state picture. The ground state $|DD\rangle$ is coherently excited by Rydberg interaction $\hat{H}_d$ with strength V_{eff}, excited state $|\zeta_{+}\rangle|\zeta_{-}\rangle$ or $|\zeta_{-}\rangle|\zeta_{+}\rangle$ spontaneously decay to ground state subspace with emission rate γ_{eff}.

It is evident that the microwave pulses facilitate a series of resonant transitions between arbitrary two states directly or indirectly within the ground-state subspace as depicted in Fig. 2(a). This means that even in the presence of incoherent spontaneous emission, no steady state appears during all the time evolution periods in presenting the 'shuffling' picture. Hence, aiming to engineer a steady state picture composed of the desired entanglement is the key requirement for establishing an entangled ground state by dissipative preparation. As illustrated in Fig. 2(b), the coherent and dissipative interactions of the ground and excited states have been visualized into the so-called steady state picture. We note that

$$|\psi_S\rangle = \frac{1}{\sqrt{\frac{1}{2}\delta^2+\omega^2}}\left(\frac{\delta}{\sqrt{2}}|00\rangle + \omega|DS\rangle\right) \tag{8}$$

is the unique steady singlet-like state of the master Eq. (6), i.e., $\hat{\rho}(t\to\infty) = |\psi_S\rangle\langle\psi_S|$. This state is equivalent to a standard KLM state by applying local operations and modulating the parameters $\delta = \sqrt{2}\omega$. To further clarify the mechanism of the state preparation explicitly, we first identify the roles of unitary dynamics and dissipative dynamics. Hamiltonian $\hat{H}_d$ in Eq. (4) corresponds to the Rydberg interaction. If the initial state is $|DD\rangle$, it would be excited to two-excitation subspace at a rate of $V_{\text{eff}} = \langle DD|\hat{H}_d|\zeta_{\pm}\zeta_{\mp}\rangle$. The Lindblad operators $\hat{\mathcal{L}}_j^0$ and $\hat{\mathcal{L}}_j^1$ may enable the population accumulation on target state $|\psi_S\rangle$ with the time evolution at a rate of $\gamma_{\text{eff}} = \langle\psi_S|\hat{\mathcal{L}}_j^0|\zeta_{\pm}\zeta_{\mp}\rangle|^2$ and $\langle\psi_S|\hat{\mathcal{L}}_j^1|\zeta_{\pm}\zeta_{\mp}\rangle|^2$, respectively. However, as the undesired states consisting of $|DD\rangle$, $|DT\rangle$, and $|\psi_1\rangle = 1/\sqrt{\frac{\delta^2}{2}+\omega^2}(\omega|00\rangle - \delta/\sqrt{2}|DS\rangle)$ are populated, the Hamiltonian $\sum_{j=1,2}\hat{H}_{\omega}^{j}$ will reshuffle the undesired states. The pumping and decay procedures will repeat again until the system reaches equilibrium, that is, the cooperation of the unitary and dissipative dynamics turns the state $|\psi_S\rangle$ into a unique steady state. This also means that the final population always tends to the state $|\psi_S\rangle$ no matter which initial state is set from evolution subspace.

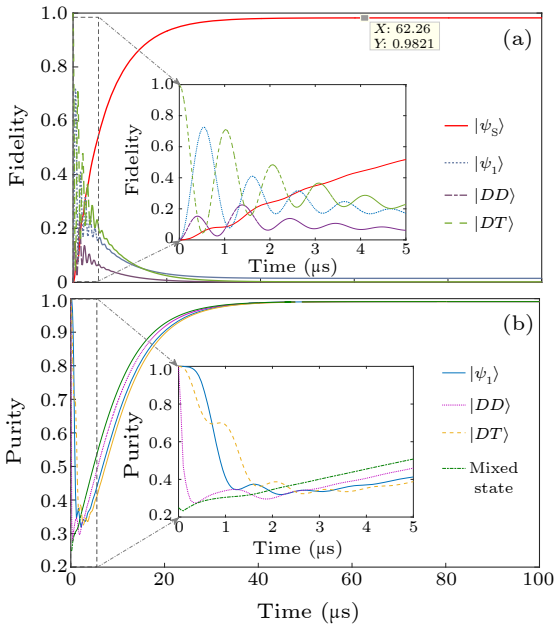

Fig. 3. (a) Population of the basis vectors in the ground-state space from the specified initial state $|DD\rangle$. (b) Purity of the target entangled state $|\psi_S\rangle$ from the different initial states $|DD\rangle$, $|DT\rangle$, $|\psi_1\rangle$, and the mixed state $(|DD\rangle + |DT\rangle + |\psi_S\rangle + |\psi_1\rangle)/4$. The insets in (a) and (b) show enlarged views of the parts indicated by the arrows, respectively. Parameters are chosen as $\Omega_1/2\pi = 20\,\text{MHz}$, $\Omega_2/2\pi = 2\Omega_1$, $\gamma_p/2\pi = 3.03\,\text{MHz}$, $\gamma_R/2\pi = 0.001\,\text{MHz}$, $\omega/2\pi = 0.25\,\text{MHz}$, $\delta = \sqrt{2}\omega$, and $V_{\text{RR}} = \Omega_1$.

Performance of the Scheme. In order to check the correctness and feasibility of our proposal, we plot the dynamical evolution of the fidelity $\mathcal{F}(t) = \langle\phi|\hat{\rho}(t)|\phi\rangle$ ($|\phi\rangle \in |DD\rangle, |DT\rangle, |\psi_1\rangle, |\psi_S\rangle$) with identical initial state $|DD\rangle$, through numerically solving the master equation [Eq. (6)] in Fig. 3(a). The results show that the fidelity of target entangled state will arrive at 98.21% after time duration $t = 62.26\,\mu\text{s}$. We also plot an enlarged view covering a

smaller range of evolution time $\in [0, 5]$ μs to visualize the dynamical process [inset of Fig. 3(a)]. Obviously, the basis vector of undesired components exhibit a coherent population oscillation and their amplitudes shrink markedly as time evolves, while the population on target entangled state is accumulated gradually. These numerical calculations are well coincident with the theoretical analysis described above. In Fig. 3(b), we simulate the purity $\mathcal{P}(t)$=Tr$[\hat{\rho}^2(t)]$ of the system with the atoms initially being in the state $|DD\rangle$, $|DT\rangle$, $|\psi_1\rangle$, and the mixed state $(|DD\rangle + |DT\rangle + |\psi_S\rangle + |\psi_1\rangle)/4$. When the system is in a purely steady state, the purity will be equal to unit, otherwise, the purity will be less than unit. We can find from the figure that all of the initial states tend to be target state $|\psi_S\rangle$ in the same way of evolution, and the purity is around 99% at $t = 62.26\,\mu$s. This means that the system will eventually reach a unique steady state regardless of whether the system is initially in purity or mixed state. In the inset of Fig. 3(b), the evolution curves display valleys within the evolutive range 0.5 μs. This is due to the fact that the coherent driving is dominant in the early stage of evolution, leading to the system to be in a mixture of a variety of quantum states. With the increase of evolution time, the competition between the coherent driving and dissipation reaches a balance.

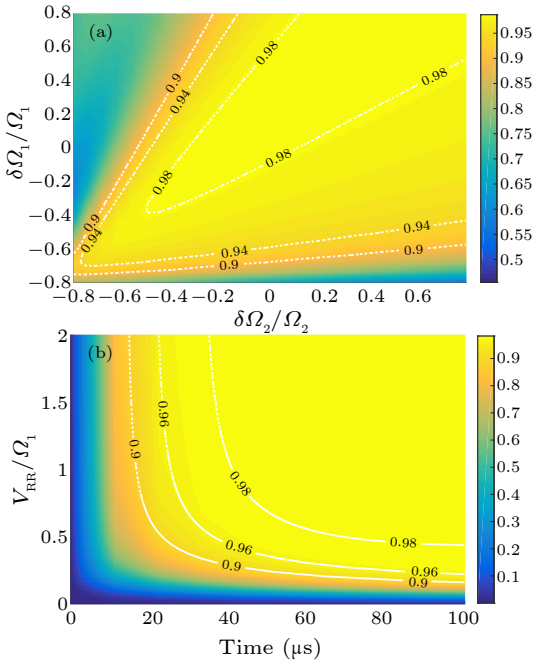

Fig. 4. (a) Contour plot of steady-state fidelity on the relative fluctuations $\delta\Omega_1/\Omega_1$ and $\delta\Omega_2/\Omega_2$. (b) Fidelity of state $|\psi_S\rangle$ as functions of evolution time and Rydberg interaction strength V_{RR}/Ω_1. The rest of the parameters are the same as those in Fig. 3.

In view of experimental scenarios, it is impossible to avoid the potential operation inaccuracy and the system instability. One can numerically evaluate robustness of the scheme against the stochastic fluctuations by defining a relative deviation as $\delta\Omega/\Omega$ with $\delta\Omega$ being the real value away from the optimum. In Fig. 4(a), we investigate the steady-state fidelity $\mathcal{F}(\hat{\rho}_\infty) = \langle\psi_S|\hat{\rho}_\infty|\psi_S\rangle$ of target state as functions of $\delta\Omega_1/\Omega_1$ and $\delta\Omega_2/\Omega_2$. The dashed lines represent some contours of the fidelity above 90%. The figure forcefully proves that the fidelity is influenced faintly even when the related parameters are suffered from 20% deviation. In addition, the Rydberg interaction between two Rydberg atoms is particularly utilized here as a pumping source to drive the undesired states in the ground-state subspace to that in two-excitation subspace. However, the Rydberg interaction is generally sensitive to atomic motion, finite laser linewidth, and the external magnetic field, which may give rise to the dephasing and decay of Rydberg atoms during the optical pumping. Therefore, we consider how the variation of the Rydberg interaction strength V_{RR} affects the population evolution of target state observed in Fig. 4(b). From this figure we find that the convergence rate towards the steady state is almost insensitive to strong interaction regime, i.e., $V_{RR} \geq \Omega_1$, and the steady-state fidelity remains higher than 0.98. Otherwise, a longer timescale for scheme implementation is required, and an intuitive explanation of this result is that the lower pumping frequency will lead to the slower preparation efficiency inevitably. Even then, it is possible to generate a high quality steady-state entanglement for a wide range of control parameters in realistic operation.

According to the long-range interaction between Rydberg atoms, certain specific states are pumped by using the interaction different from Rydberg blocking and anti-blocking effects. In order to achieve this, such an effect is combined with quantum dissipation. In this scheme, the transition process caused by the microwave field is combined with the pumping process caused by the Rydberg interaction. This leads to the resonance transformation of the undesired state into the double-excited Rydberg state, and the double-excited Rydberg state will decay to the desired state with a specific probability through dissipation. This scheme thus forms a closed cycle, so that all states except the KLM state will be driven and decay again.

In summary, we have discussed the effective method to prepare the two-atom maximal entanglement based on the dissipative EIT and Rydberg pumping regimes. According to the obtained results, it is found that this method does not require initial state and precise control of evolution time, compared to other dissipative entangled state preparation schemes. In addition, the method can also achieve higher fidelity and shorter convergence time. Based on these results, we believe that this method can provide a better theoretical scheme for preparing bipartite KLM entangled state.

Acknowledgements. This work was supported by the LiaoNing Revitalization Talents Program (Grant No. XLYC1907033), the Natural Science Foundation of Liaoning Province (Grant No. 2023-MS-072), the National Natural Science Foundation of China (Grant No. 11905027), and the Fundamental Research Funds for the Central Universities (Grant Nos. N2209005 and N2205015).

References

[1] Ketterle W 2002 *Rev. Mod. Phys.* **74** 1131
[2] Nadlinger D P, Drmota P, Nichol B C, Araneda G, Main D, Srinivas R, Lucas D M, Ballance C J, Ivanov K, Tan E

Y, Sekatski P, Urbanke R L, Renner R, Sangouard N, and Bancal J D 2022 *Nature* **607** 682
[3] Ekert A K 1991 *Phys. Rev. Lett.* **67** 661
[4] Ashhab S, Maruyama K, Brukner Č, and Nori F 2009 *Phys. Rev. A* **80** 062106
[5] Heaney L, Lee S W, and Jaksch D 2010 *Phys. Rev. A* **82** 042116
[6] Xue P, Xiao L, Ruffolo G, Mazzari A, Temistocles T, Terra C M, and Rabelo R 2023 *Phys. Rev. Lett.* **130** 040201
[7] Bouwmeester D, Pan J W, Mattle K, Eibl M, and Zeilinger A 1997 *Nature* **390** 575
[8] Braunstein S L and Kimble H J 1998 *Phys. Rev. Lett.* **80** 869
[9] Schuch N, Verstraete F, and Ignacio C J 2004 *Phys. Rev. A* **70** 042310
[10] Heaney L and Vedral V 2009 *Phys. Rev. Lett.* **103** 200502
[11] Mattle K, Weinfurter H, and Kwiat P G 1996 *Phys. Rev. Lett.* **76** 4656
[12] Li X Y, Pan Q, Jing J T, Zhang J, Xie C D, and Peng K C 2002 *Phys. Rev. Lett.* **88** 047904
[13] Kimble H 2008 *Nature* **453** 1023
[14] Knill E, Laflamme R, and Milburn G J 2001 *Nature* **409** 46
[15] Zheng R H, Xiao Y, Su S L, Chen Y H, Shi Z C, Song J, Xia Y, and Zheng S B 2021 *Phys. Rev. A* **103** 052402
[16] Shao X Q, Wu J H, Yi X X, and Long G L 2017 *Phys. Rev. A* **96** 062315
[17] Zheng S B 2001 *Phys. Rev. Lett.* **87** 230404
[18] Franson J D, Donegan M M, and Jacobs B C 2004 *Phys. Rev. A* **69** 052328
[19] Cheng L Y, Wang H F, Yeon K H, and Zhang S 2012 *J. Opt. Soc. Am. B* **29** 1584
[20] Ji Y Q, Li H, Liu Y L, Zhang D W, Zhou X J, Xiao R J, Dong L, and Xiu X M 2020 *Laser Phys. Lett.* **17** 085202
[21] Li D X, Shao X Q, Wu J H, Yi X X 2017 *Opt. Express* **25** 33359
[22] Sheng Y B, Deng F G, and Zhou H Y 2008 *Phys. Rev. A* **77** 042308
[23] Millo O, Katz D, and Cao Y W 2001 *Phys. Rev. Lett.* **86** 5751
[24] Shi J 2019 *J. Phys. B* **52** 01LT01
[25] Wang Y, Hu C S, Shi Z C, Huang B H, Song J, and Xia Y 2019 *Ann. Phys.* **531** 1900006
[26] Liu Q G, Wu Q C, and Ji X 2014 *J. Opt. Soc. Am. B* **31** 672
[27] Zheng R H, Kang Y H, Ran D, Shi Z C, and Xia Y 2020 *Phys. Rev. A* **101** 012345
[28] Haase T, Alber G, and Stojanović V M 2021 *Phys. Rev. A* **103** 032427
[29] Nielsen M A and Chuang I L 2010 *Quantum Computation and Quantum Information* (Cambridge: Cambridge University Press)
[30] Aolita L, de Melo F, and Davidovich L 2015 *Rep. Prog. Phys.* **78** 042001
[31] Poyatos J F, Cirac J I, and Zoller Z 1996 *Phys. Rev. Lett.* **77** 4728
[32] Plenio M B and Huelga S F 2002 *Phys. Rev. Lett.* **88** 197901
[33] Zou J, Zhang S, and Tserkovnyak Y 2022 *Phys. Rev. B* **106** L180406
[34] Cole D C, Wu J J, Erickson S D, Hou P Y, Wilson A C, Leibfried D R F 2021 *New J. Phys.* **23** 073001
[35] Shao X Q, Zheng T Y, Oh C H, and Zhang S 2014 *Phys. Rev. A* **89** 012319
[36] Su S L, Shao X Q, Wang H F, and Zhang S 2014 *Sci. Rep.* **4** 7566
[37] Reiter F, Reeb D, and Sørensen A S 2016 *Phys. Rev. Lett.* **117** 040501
[38] Song J, Xia Y, Sun X D, and Song H S 2012 *Phys. Rev. A* **86** 034303
[39] De Moraes N S D, Teizen V F, Montenegro V, and Vernek E 2017 *Phys. Rev. A* **96** 062313
[40] Shao X Q, Wang Z H, Liu H D, and Yi X X 2016 *Phys. Rev. A* **94** 032307
[41] Sweke R, Sinayskiy I, and Petruccione F 2013 *Phys. Rev. A* **87** 042323
[42] Shen L T, Chen X Y, Yang Z B, Wu H Z, and Zheng S B 2011 *Phys. Rev. A* **84** 064302
[43] Berkley J A 2003 *Science* **300** 1548
[44] DiCarlo L 2010 *Nature* **467** 574
[45] Politi A, Matthews J C F, and O'Brien J L 2009 *Science* **325** 1221
[46] Akopian N, Lindner N H, Poem E, Berlatzky Y, Avron J, Gershoni D, Gerardot B D, and Petroff P M 2006 *Phys. Rev. Lett.* **96** 130501
[47] Yin J, Cao Y, Li Y H *et al.* 2017 *Science* **356** 1140
[48] Balasubramanian G, Neumann P, and Twitchen D 2009 *Nat. Mater.* **8** 383
[49] Xue P and Xiao Y F 2006 *Phys. Rev. Lett.* **97** 140501
[50] Brion E, Pedersen L H, and Molmer K 2007 *Phys. Rev. A* **75** 032328
[51] Blatt R and Wineland D 2008 *Nature* **453** 1008
[52] Saffman M, Walker T G, and Mlmer K 2010 *Rev. Mod. Phys.* **82** 2313
[53] Saffman M and Walker T G 2005 *Phys. Rev. A* **72** 042302
[54] Shi X F 2020 *Phys. Rev. Appl.* **13** 024008
[55] Weimer H, Müller M, Lesanovsky I, Zoller P, B, and Hans P 2010 *Nat. Phys.* **6** 382
[56] Ren J G 2017 *Nature* **549** 70
[57] Montanaro A and Pallister S 2016 *Phys. Rev. A* **93** 032324
[58] Mølmer K, Isenhower I, and Saffman M 2011 *J. Phys. B* **44** 184016
[59] Li R, Yu D M, Su S L, and Qian J Q 2020 *Phys. Rev. A* **101** 042328
[60] Su S L and Li W B 2021 *Phys. Rev. A* **104** 033716
[61] Chen Y H, Shi Z C, Song J, Xia Y, and Zheng S B 2018 *Phys. Rev. A* **97** 032328
[62] Walker T G and Saffman M 2008 *Phys. Rev. A* **77** 032723
[63] Li D X and Shao X Q 2019 *Phys. Rev. A* **99** 032348